ELSEVIER

Reversible mesoscopic model of protein adsorption: From equilibrium to dynamics

G.J. Szöllősi[a,*], I. Derényi[a], J. Vörös[b]

[a]*Department of Biological Physics, Eötvös University, Pázmány P. stny. 1A, H-1117 Budapest, Hungary*
[b]*BioInterface Group, Laboratory for Surface Science and Technology, ETH Zürich, Wagistrasse 2, 8952 Schlieren, Switzerland*

Abstract

We present a thermodynamically consistent mesoscopic model of protein adsorption at liquid–solid interfaces. First describing the equilibrium state under varying protein concentration of the solution and binding conditions, we predict a non-trivial (non-monotonic) dependence of the experimentally observable properties of the adsorbed layer (such as the surface density and surface coverage) on these parameters. We subsequently proceed to develop a dynamical model consistent with the equilibrium description, which qualitatively reproduces known experimental phenomena and offers a promising way of studying the exchange of the adsorbed proteins by the proteins of the solution.
© 2004 Elsevier B.V. All rights reserved.

1. Introduction

Protein adsorption at liquid–solid interfaces is a fundamental problem of several diverse areas of biotechnology. A short list would include, biocompatibility of

---

*Corresponding author.

  E-mail address: ssolo@angel.elte.hu (G.J. Szöllősi).

implants, blood clotting, filter fouling and protein chip technology. It is also a problem of general theoretical interest, especially because despite the considerable body of experimental data and empirical phenomena—due in part to the very precise methods available for the measurement of the adsorbed amount—the literature is thus far lacking a mesoscopic (particle level) description that can account for all of the experimental observations [1]. Below we present a model that will—we hope—not only meet the above criteria, but do so in a physically consistent manner.

The basic treatise behind various particle level descriptions of protein adsorption is that adsorbed proteins can be in several different states of different surface (or footprint) sizes. This is supported by experimental evidence that adsorbed proteins undergo surface-induced conformational change [2–4] characterized by a substantial growth of the surface contact area. Combined with evidence [5] that under conditions of high surface coverage these transitions are sterically hindered by neighboring proteins on the surface, the usual mesoscopic description is completed by assuming a hard-core repulsive interaction between proteins—both on the surface and in the solution.

Although proteins adsorb to a two-dimensional (2D) substrate, we will further use a one-dimensional (1D) approximation. This simplification is justified, on one hand, by the fact that there is no thermodynamic phase transition (which is usually sensitive to the dimensionality) in the adsorption process, and on the other hand, because the main features of adsorption (such as jamming, slow convergence toward equilibrium, short-range spatial correlations) are independent of the spacial dimensions. 1D models already have the ingredients that make their behavior non-trivial and qualitatively similar to that observed in higher dimensions, and they are much easier to treat analytically [6].

Surface-protein systems of interest typically exhibit tightly bound protein states with binding energies upto several tens of $k_B T$ [7]. This is the reason that most models to date have incorporated at least partial irreversibility to explain the obvious deviation of protein adsorption from simple Langmuir-like behavior [8]. The classical irreversible model of particle adsorption, random sequential adsorption (RSA) (for a recent review see Ref. [6]), in which adsorption is considered to be permanent and the adsorbed system of particles on the surface is eventually described by a jammed state with no more free space available for particle deposition, is inherently incapable of describing any process involving desorption of proteins. The second class of models [9–13] differentiate between reversibly adsorbed states of small size and irreversibly adsorbed larger states. These models rely on the assumption that the escape from the strongly bound states is practically impossible under reasonable experimental time scales. This notion is supported by the experimental evidence of long relaxation times of the observed properties. We show that slow relaxation of experimental observables (typically surface density) can be equally well described by a reversible model, and that such an approach has a non-trivial equilibrium state distribution, with several unprecedented predictions for the concentration and binding strength dependence of the surface density and the surface coverage, respectively. We also argue that exchange effects, widely observed for non-biological polymers [14], and to a limited extent for proteins [15] can only be treated in the context of a reversible model such as ours.
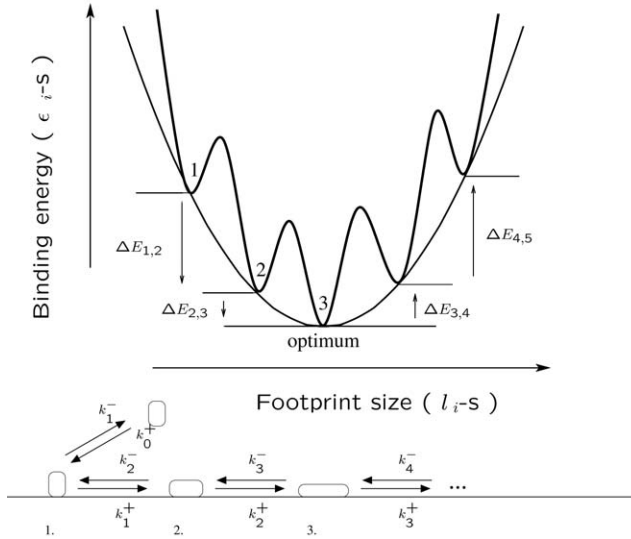
Fig. 1. Adhesion potential of a protein, where each of its states i (characterized by a binding energy ε_i and a footprint size l_i) is separated from the neighboring states by potential barriers. The corresponding transition rates are $k_i^{\pm}$ (defined in Section 3).

2. Equilibrium model

In our model we consider a 1D line of adsorption of size L in contact with a protein solution of constant concentration c. Each protein being adsorbed on this line is considered to be in one of M different states, each characterized by an ε_i binding energy ($1 \leqslant i \leqslant M$) and a monotonically increasing[1] l_i linear footprint size (see Fig. 1). Proteins in the smallest footprint state ($i = 1$) can undergo adsorption from and desorption to the protein solution, characterized by a k_a adsorption and a k_d desorption rate. Adsorption and desorption in other states are neglected, because these states have lower energies on the surface and higher energies in the solution than those of the smallest footprint state, and thus, represent much slower adsorption–desorption kinetics. Proteins interact via a hard-core repulsion, i.e., they are not allowed to overlap.

Given a set of values for the parameters $(L, c, \{\varepsilon_i\}, \{l_i\}, k_a, k_d)$ the model has a unique equilibrium distribution of states $\{n_i\}$, where n_i denotes the number of adsorbed proteins in state i, and

$$\sum_{i=1}^{M} n_i = N \tag{1}$$

[1] We can assume $\{l_i\}$ to be monotonically increasing as for any set of $\{l_i\}$ and $\{\varepsilon_i\}$ we can obtain this by appropriately rearranging the $\{l_i\}$-s, because there is no constraint on the $\{\varepsilon_i\}$-s.

is the total number of proteins adsorbed on the surface. The distribution must obey the

$$\sum_{i=1}^{M} n_i l_i \leqslant L \tag{2}$$

spatial constraint. Our reversible dynamical models (defined later) will be explicitly shown to converge to this equilibrium distribution.

2.1. The conditional free energy

The above equilibrium distribution can be obtained by determining the conditional free energy

$$F(\{n_i\}) = E(\{n_i\}) - TS(\{n_i\}) - \mu N(\{n_i\}) \tag{3}$$

for any given distribution $\{n_i\}$ (obeying the spatial constraint), and finding the distribution $\{n_i^{min}\}$ which minimizes it. The energy $E(\{n_i\})$ and the entropy $S(\{n_i\})$ can be expressed as

$$E(\{n_i\}) = \sum_{i=1}^{M} \varepsilon_i n_i \quad \text{and} \quad S(\{n_i\}) = -k_B \ln C(\{n_i\}) \tag{4}$$

and N is given by Eq. (1). Now we need to count the number of possible arrangements (configurations) $C(\{n_i\})$ of the proteins on the surface, and express the chemical potential μ of the proteins in the solution in terms of their concentration and adsorption/desorption rates. Restricting ourselves to a 1D model has the advantage that the number of configurations $C(\{n_i\})$ can be calculated in a straightforward manner.

2.1.1. Adsorption on a lattice

Representing the surface as a 1D lattice of period δ (with L/δ sites), the problem of calculating $C(\{n_i\})$ reduces to a simple combinatoric exercise. Denoting the total occupied surface as

$$l = \sum_{i=1}^{M} n_i l_i \tag{5}$$

and the number of unoccupied lattice sites as

$$n_0 = \frac{L - l}{\delta} , \tag{6}$$

the number of different permutations of the N adsorbed proteins and the n_0 empty sites is $(n_0 + N)!$. Since proteins in the same state, as well as the empty sites are indistinguishable, this has to be divided by $n_0! \prod_{i=1}^{M} n_i!$ to get the number of different

configurations:

$$C(\{n_i\}) = \frac{(n_0 + N)!}{n_0! \prod_{i=1}^{M} n_i!} \; . \tag{7}$$

Considering the lattice constant δ small compared to the protein footprint size implies that the number of empty sites is much larger than N. Consequently, in the above formula we can make the approximation:

$$\frac{(n_0 + N)!}{n_0!} \simeq n_0^N \; , \tag{8}$$

which is shown to be exact as $\delta \to 0$, in the Appendix.

Using Stirling's formula and neglecting the sub-linear terms in N:

$$\ln C(\{n_i\}) \simeq \left(N \ln \frac{L-l}{\delta} - \sum_{i=1}^{M} n_i \ln n_i + N \right) . \tag{9}$$

The entropy can now be written as

$$S(\{n_i\}) = k_B N \ln \frac{L-l}{\delta} - k_B \sum_{i=1}^{M} n_i \ln n_i + k_B N \; . \tag{10}$$

Introducing the state densities

$$\rho_i = \frac{n_i}{L} \quad \text{and} \quad \rho = \sum_{i=1}^{M} \rho_i = \frac{N}{L} \tag{11}$$

for proteins in state i and for the total adsorbed proteins, respectively, as well as the corresponding fractional surface coverages

$$\lambda_i = \frac{l_i n_i}{L} \quad \text{and} \quad \lambda = \sum_{i=1}^{M} \lambda_i = \sum_{i=1}^{M} \rho_i l_i = \frac{l}{L} \; , \tag{12}$$

we can explicitly express the extensivity of the entropy or equivalently the lack of dependence of the entropy density $s = S/L$ on the system size L, by writing the entropy density as

$$s(\{\rho_i\}) = \frac{S(\{L\rho_i\})}{L} = k_B \left(\rho \ln(1 - \lambda) - \rho \ln \delta - \sum_{i=1}^{M} \rho_i \ln \rho_i + \rho \right) . \tag{13}$$

The chemical potential can be derived from the requirement that for a system in equilibrium detailed balance must hold. In our case this requirement prescribes that the rate of adsorption to a particular site per unit time, $\delta c k_a$, and the rate of desorption from the same state, k_d, satisfy

$$\exp\left(\frac{\mu_\delta - \varepsilon_1}{k_B T} \right) = \frac{\delta c k_a}{k_d} \tag{14}$$

yielding

$$\mu_\delta = \underbrace{\underbrace{\varepsilon_1 + k_B T \ln \frac{k_a}{k_d}}_{\mu_0} + k_B T \ln c}_{\mu} + k_B T \ln \delta = \mu + k_B T \ln \delta , \qquad (15)$$

where we have separated μ into μ_0 (which depends only on the binding conditions) and $k_B T \ln c$ (which depends on the concentration). For the sake of brevity we will consider $k_B T = 1$ throughout the paper. We can then write the conditional free energy density using (3), (13) and (15) as

$$\phi(\{\rho_i\}) = \frac{F(\{L\rho_i\})}{L} = \sum_{i=1}^{M} \rho_i \varepsilon_i - \rho(1 + \mu) - \rho \ln(1 - \lambda) + \sum_{i=1}^{M} \rho_i \ln \rho_i , \qquad (16)$$

where the $\ln \delta$ terms have canceled, and hence, the free energy density is independent of the spatial resolution δ.

2.2. Equilibrium state distribution

The free energy density (16) can be formally extremized by solving

$$\frac{\partial \phi(\{\rho_i\})}{\partial \rho_i} = \varepsilon_i - \mu + \ln \rho_i - \ln(1 - \lambda) + \frac{\rho}{1 - \lambda} l_i = 0 . \qquad (17)$$

This yields for the equilibrium state density distribution

$$\rho_j = (1 - \lambda) e^\mu e^{-(\varepsilon_j + \rho/(1-\lambda)l_j)} , \qquad (18)$$

which must satisfy the self-consistency criteria:

$$\rho = \sum_{i=1}^{M} \rho_i \quad \text{and} \quad \lambda = \sum_{i=1}^{M} l_i \rho_i . \qquad (19)$$

To numerically solve the above we can proceed by defining the functions

$$\rho^*(\rho, \lambda) = \sum_{i=1}^{M} \rho_i^*(\rho, \lambda) \qquad (20)$$

and

$$\lambda^*(\rho, \lambda) = \sum_{i=1}^{M} l_i \rho_i^*(\rho, \lambda) , \qquad (21)$$

where

$$\rho_i^*(\rho, \lambda) = (1 - \lambda) e^\mu e^{-(\varepsilon_i + \rho/(1-\lambda)l_i)} . \qquad (22)$$

For a given set of values of the parameters $(c, \{\varepsilon_i\}, \{l_i\}, k_a, k_d)$,

$$\rho^*(\rho, \lambda) - \rho = 0 \quad \text{and} \quad \lambda^*(\rho, \lambda) - \lambda = 0 \qquad (23)$$

define two curves in the (ρ, λ)-space, an intersection of which (at the point $\rho = \rho^{\text{ext}}$ and $\lambda = \lambda^{\text{ext}}$) gives a solution of Eq. (17). Provided that $\rho^{\text{ext}} \in [0, 1/(\min\{l_i\})]$ and $\lambda^{\text{ext}} \in [0, 1]$, this corresponds to an extremum of the conditional free energy (16),

$$\rho_i^{\text{ext}} = (1 - \lambda^{\text{ext}})e^{\mu}e^{-(\varepsilon_i + \rho^{\text{ext}}/(1-\lambda^{\text{ext}})l_i)} \ . \tag{24}$$

From physical considerations it is obvious that there must be at least one such solution, which is furthermore a minimum of (16) (otherwise we would be left without a stable equilibrium state). Although a formal proof is so far lacking, numerical results indicate that there are no values of the parameters for which there would be more than one solution.

2.3. Linear approximation

If we only wish to gain information on whether, for a particular system, the proteins adsorbed on the surface spread out completely (energy dominated regime), or whether they remain compact despite the availability of energetically favorable but larger states (entropy dominated regime), we can proceed by considering a simple linear approximation for the binding energies as a function of the footprint size, and neglect all higher order terms:

$$\varepsilon_i = \varepsilon l_i \ . \tag{25}$$

It is immediately apparent that Eq. (24) specifies an exponential form for the equilibrium state density distribution:

$$\rho_j = \underbrace{(1 - \lambda)e^{\mu}}_{b}\overbrace{e^{-(\varepsilon + \rho/(1-\lambda))}}^{a}{}^{l_j} = be^{al_j} \ . \tag{26}$$

This result of an exponential state density distribution then, depending on the exponent a, corresponds either to a system—for negative a—where proteins remain compact compared to their energetically more favorable (assuming $\varepsilon < 0$) spread out state, or—for positive a—to a system where they spread out and predominantly occupy their lowest energy state. Within the context of our approximation the crossover between these two modes of behavior can be analytically derived. Since for $a = 0$, $\rho_i = b$ the self-consistency criteria (19) become independent of the ρ_i-s:

$$\rho = \sum_{i=1}^{M} \rho_i = bM \quad \text{and} \quad \lambda = \sum_{i=1}^{M} \rho_i l_i = b\sum_{i=1}^{M} l_i \ . \tag{27}$$

Substituting for ρ in the definition $a = -(\varepsilon + \rho/(1 - \lambda))$ and setting it equal to zero we obtain

$$(1 - \lambda)\varepsilon = -bM \ . \tag{28}$$

Using the definition $b = e^{\mu}(1 - \lambda)$ we arrive at

$$e^{\mu} = -\frac{\varepsilon}{M} \ . \tag{29}$$

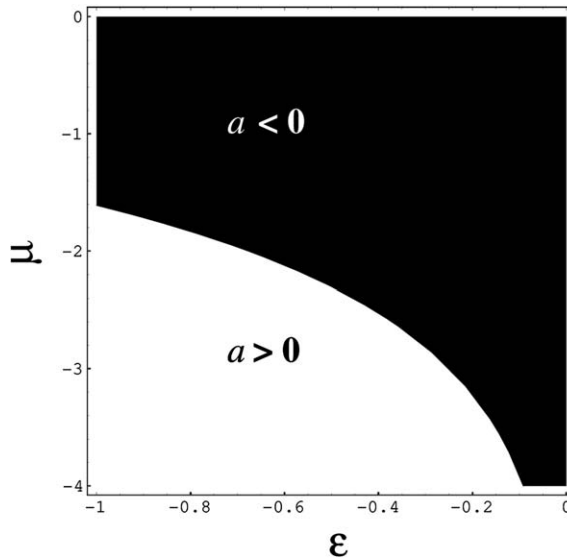Fig. 2. Plot in (ε, μ)-space of the $a = 0$ contour for $M = 5$ and $l_i = i$.

We can see that for a given value of $\varepsilon < 0$ there is always a value of μ and consequently c below which the proteins spread out and the system is characterized by a low surface density but high surface coverage ($a > 0$), and above which the surface density is high but the proteins are relatively loosely adhered ($a < 0$) (see Fig. 2 as an example).

Considering the number and size of the subsequent footprints $\{l_i\}$ immutable, the equilibrium state of the adsorbed proteins can be completely determined for any given value of ε and μ. We can then plot the values of a, ρ or λ in the (ε, μ) parameter space and visualize the effect of varying the chemical potential (i.e., changing the concentration) or the adhesion energy (i.e., changing either the adsorbing protein or the surface [16,17]) for a given system.[2] The change of sign of a in the (ε, μ)-space corresponds, as shown in Eq. (29) to the curve $\mu = \ln(-\varepsilon/M)$ (Fig. 2). This result is independent of the choice of $\{l_i\}$-s. An examination of the unit surface coverage λ shows a non-monotonic μ (or $\ln c$) vs. λ dependence (Fig. 3 a, c, and e) characterized by a maximum and a minimum, while the total surface density ρ demonstrates similar unexpected non-monotonic behavior exhibiting a maximum in ε (Fig. 3 b, d, and e). Experimental evidences for this latter behavior can be found in Ref. [18], where the saturation level of the adsorbed amount of various proteins (HSA, hFb) showed a non-monotonic dependence on the grafting ratio of PEG chains on TiO_2 surfaces.

---

[2]The chemical potential as defined by Eq. (15) also depends through μ_0 on ε as well as k_d and k_a which probably depend on ε as interpreted above, but a pure $\ln c$ vs. ε plot can be recovered from the $\mu_0 + \ln c$ vs. ε results by a transformation of the coordinates.
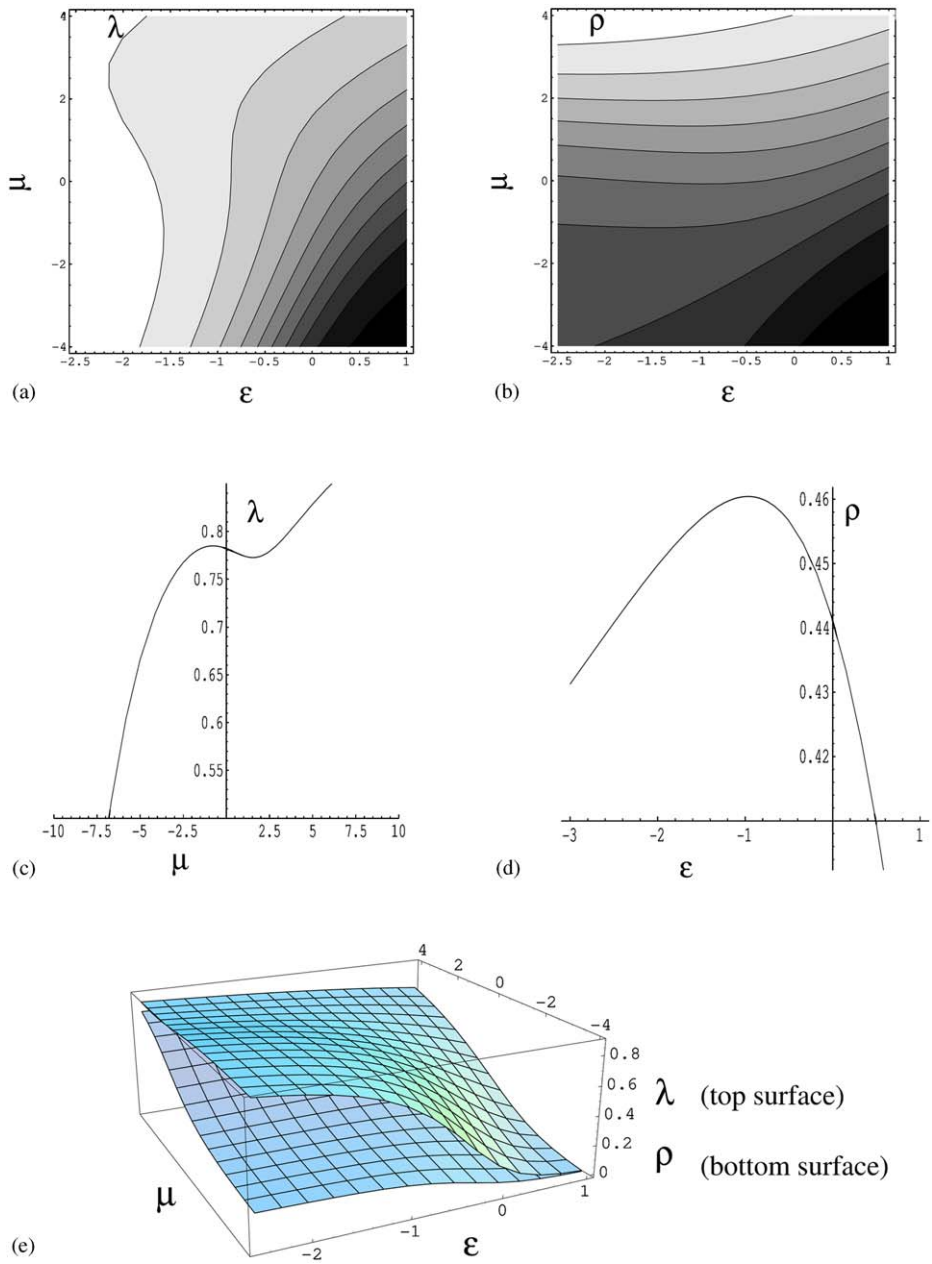
Fig. 3. (a) and (b) contours of λ and ρ in the (ε, μ)-space, (c) and (d) slices of λ along μ at $\varepsilon = -1.2$ and ρ along ε at $\mu = 1$, (e) surface plot of λ and ρ together, for $M = 5$ and $l_i = i$ throughout.

2.4. Non-linear potentials

For potentials with non-linear footprint size dependence, the equilibrium state density distribution can be calculated numerically just as easily as for the preceding linear case. The solution, on the other hand, is no longer a simple exponential distribution and the potential cannot be as easily parameterized in a physically meaningful manner.

3. Dynamics

In the following we introduce two limiting cases of a general dynamics, both of which minimize the free energy density (16). In these models we consider thermodynamically consistent rates for the transitions of a protein between neighboring states and for the adsorption and desorption of the protein from and to the smallest footprint state. These rates are derived from a potential for which each state is separated by a potential barrier (Fig. 1). Consequently, the rate of a protein expanding from state i (for $1 \leqslant i < M$) to state $i + 1$ (presuming there is sufficient adjacent empty space) is

$$k_i^+ = v_i e^{-\Delta E_{i+1,i}/2k_B T}, \tag{30}$$

while the rate of shrinking from state i (for $1 < i \leqslant M$) to $i - 1$ is

$$k_i^- = v_{i-1} e^{-\Delta E_{i-1,i}/2k_B T}, \tag{31}$$

where $\Delta E_{i+1,i} = \varepsilon_{i+1} - \varepsilon_i$ and v_i is determined by the height of the energy barrier. These rates satisfy detailed balance by construction. The rate of desorption from state 1 is given as

$$k_1^- = k_d, \tag{32}$$

while the adsorption rate per unit length (into state 1) is

$$k_0^+ = k_a c. \tag{33}$$

To complete a dynamical model we must also have information on the available surface surrounding each protein at any given time as well as on the diffusion of proteins along the surface.

3.1. The infinite diffusion limit

If the diffusion of adsorbed proteins on the surface is considered infinitely fast (ideal mixing) we can construct a mean field-like model where every protein on the surface is presumed to "feel" the same environment. Defining the state density currents (i.e., the number of transitions per unit time and length) $j_i^{\pm}$ according to Fig. 4, we can see that every j_i^- (corresponding to shrinking and desorption) is independent of the protein environment, whereas every j_i^+ (corresponding to spreading and adsorption) depends on the adjacent free space, which is considered to
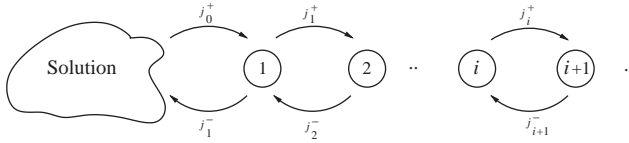
Fig. 4. The complete set of the state density currents $j_i^\pm$.

be identical for each protein in our mean field-like model. These currents then have to include the probability of finding a sufficiently large empty interval to either side. Since we assume the proteins to be perfectly mixed, the distribution of empty intervals is exponential with a mean value of $(L-l)/N = (1-\lambda)/\rho$, whence the probability of finding an interval with a size of at least x is then

$$P(x) = e^{-x(\rho/(1-\lambda))}. \tag{34}$$

Thus, we can write the state density currents as

$$\left.\begin{array}{l} j_{i+1}^- = \rho_{i+1}k_{i+1}^- = \rho_{i+1}k_{i+1}^- \\ j_i^+ = \rho_i k_i^+ P(l_{i+1}-l_i) = \rho_i k_i^+ e^{-(l_{i+1}-l_i)\rho/(1-\lambda)} \end{array}\right\} \quad i \geqslant 1 \tag{35}$$

and

$$\left.\begin{array}{l} j_1^- = \rho_1 k_d = \rho_1 k_d \\ j_0^+ = \rho_0 k_a P(l_1) = \rho_0 k_a e^{-l_1\frac{\rho}{1-\lambda}} \end{array}\right\} \quad i = 0\,. \tag{36}$$

Having derived the currents $j_i^\pm$, our system can be completely described by the following M differential equations:

$$\dot\rho_i = -(j_i^+ + j_i^-) + (j_{i-1}^+ + j_{i+1}^-) \quad 1 \leqslant i \leqslant M, \tag{37}$$

which can be readily solved numerically (as an example see Fig. 5a).

To verify whether this dynamics converges to the equilibrium state distribution, characterized by the minimum of the conditional free energy (16), let us calculate the rate of the change of this free energy if proteins in state i start to expand to state $i+1$ (for $1 \leqslant i < M$):

$$\frac{\partial\phi}{\partial\rho_{i+1}} - \frac{\partial\phi}{\partial\rho_i} = (\varepsilon_{i+1}-\varepsilon_i) + \ln\frac{\rho_{i+1}}{\rho_i} + \frac{\rho}{1-\lambda}(l_{i+1}-l_i)\,. \tag{38}$$

This quantity is identical to

$$\ln\frac{j_{i+1}^-}{j_i^+} = \underbrace{\ln\frac{k_{i+1}^-}{k_i^+}}_{\varepsilon_{i+1}-\varepsilon_i} + \ln\frac{\rho_{i+1}}{\rho_i} + \frac{\rho}{1-\lambda}(l_{i+1}-l_i)\,, \tag{39}$$

which means that expansion (j_i^+) is faster than shrinking (j_{i+1}^-) only if the rate of the free energy change for expansion is negative. A very similar derivation holds for the relation between the adsorption (j_0^+) and desorption (j_1^-) currents. Thus indeed, the currents between any two states point to a descending direction on the free energy landscape, driving the system to equilibrium.
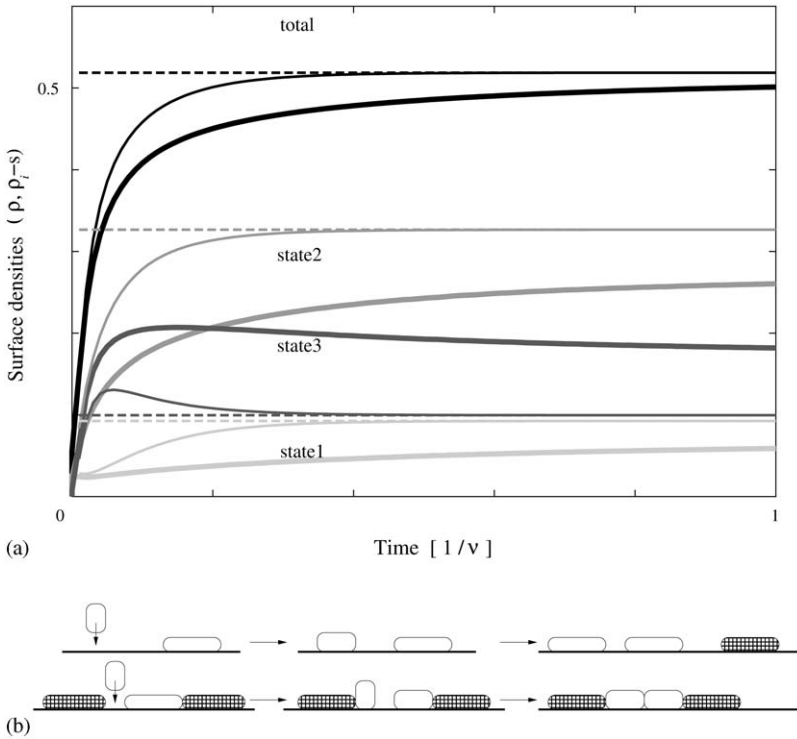
Fig. 5. (a) MC simulation of a protein-surface system with $M = 3$ possible states of sizes $l_1 = 1$, $l_2 = 1.5$, and $l_3 = 2$ with binding energies $\varepsilon_1 = -11.25\ k_B T$, $\varepsilon_2 = -14.0625\ k_B T$, and $\varepsilon_2 = -15\ k_B T$, respectively. The states are separated by barriers of equal height, characterized by a state independent $v_i = v$ prefactor in the corresponding transition rates, as defined in Eqs. (30) and (31). The desorption rate k_1^- is also given by Eq. (31) with the hypothetical ε_0 assumed to be 0. The adsorption rate is set to $k_0^+ = vc$ with a dimensionless protein concentration of $c = 0.2$. The simulation was conducted with a system of size $L = 200$ and averaged over 10000 runs. The state densities from the MC simulations (thick lines) as a function of time (measured in units of $1/v$) are plotted together with the equilibrium distribution (using Eq. (18)) (dashed lines) and the numerical solution in the infinite diffusion limit (Eq. (37)) (thin lines). The gray levels (starting from light gray) correspond to ρ_1, ρ_2, ρ_3, and ρ. (b) Sketches of different regimes of the dynamics: under low surface coverage all adsorbed proteins spread out to their energetically most favorable state (top row), while for high coverage—assuming a convex potential—the equally, but not fully spread out state may be preferential (bottom row).

3.2. The zero diffusion limit

If on the other hand we assume the proteins adsorbed on the surface immobile[3] after adsorption, we can no longer construct a mean field model such as above.

---

[3]Limited movement occurs none the less, through "crawling", i.e., successive spreading and receding of proteins resulting in movement of the particles' center of mass.

Transient effects similar to jamming in RSA begin to play a significant role, the system relaxes very slowly, and the transient state distributions can be significantly different from the eventual equilibrium. To study the zero diffusion behavior of our model we conducted Monte Carlo (MC) simulations of systems of approximately 100 proteins (system size was fixed at 100 max$\{l_i\}$) several hundred times and averaged the results. Slow relaxation and large differences in state distribution under similar total surface densities were observed (see Fig. 5) over a wide range of parameters. The simulations qualitatively reproduced several known experimental effects, such as the overshot of the surface density at high concentrations or hysteresis of the surface density as a function of the concentration even after large equilibration times. We are performing experiments which will be analyzed by such MC simulations.

3.3. Exchange

A further consequence of reversibility, aside from the subtle evolution of the state density, is the possibility of the exchange of the adsorbed proteins by the proteins of the solution (a phenomenon widely observed among simple homo-polymers [14]). To examine exchange we conducted simulations of a hypothetical setup were "labeled" proteins were allowed to adsorb for a specified time ($2/v$) and then the solution was replaced by either a buffer solution (0 c unlabeled proteins), or an "unlabeled" solution of the same concentration (1 c unlabeled proteins), or a more concentrated unlabeled solution (1000 c unlabeled proteins). Observing the concentration of labeled proteins on the surface after the introduction of the new solution (Fig. 6), we can see that the density of labeled proteins decreases faster as the concentration of unlabeled proteins is increased.

Further examining the various state densities, we see that this increase can be attributed to the labeled proteins being "ratcheted" up to smaller footprint states and eventually expelled from the surface by the newly adsorbed unlabeled proteins [15]. This is most obvious in case of the replacement with the most concentrated unlabeled solution (1000 c), where a large maximum of the surface density of state 1 (ρ_1) appears near time $2.5/v$. Since desorption occurs exclusively from this state, the inflection point (i.e., the maximal slope) of the total surface density (ρ) near the same time is another manifestation of the same ratcheting phenomenon. Because this inflection at high concentrations is a clear sign of exchange and could easily be measured, we are currently setting up similar experiments with fluorescently labeled proteins.

4. Discussion

We have presented a thermodynamically consistent model of protein adsorption possessing an equilibrium state. The existence of which facilitates the understanding and prediction of long-term effects and also offers novel predictions for the dependence of the equilibrium surface density (ρ) and surface coverage (λ) on the
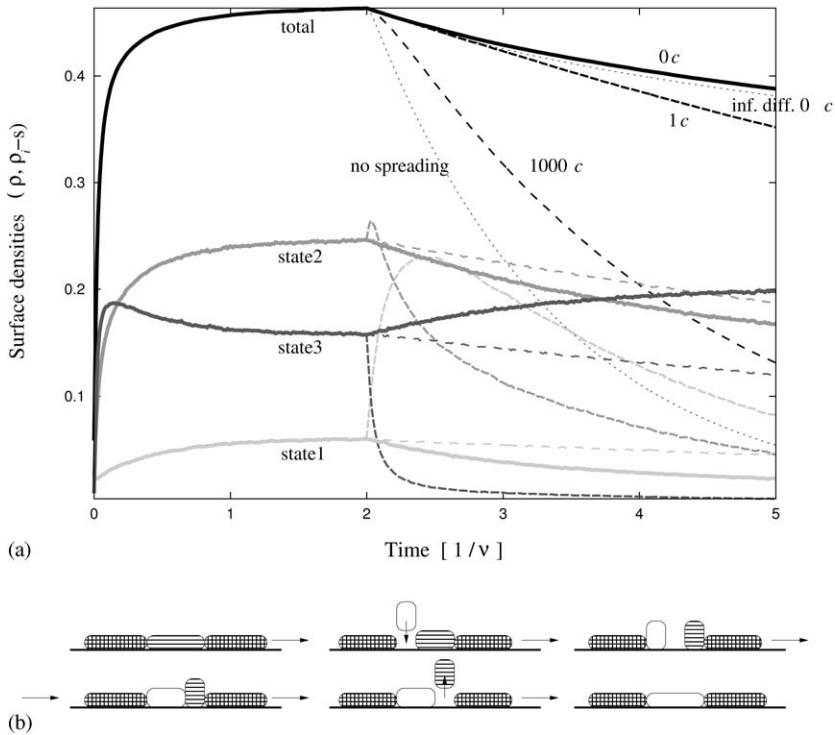
Fig. 6. (a) Plot of the state densities of "labeled" proteins from the MC simulations of the system described in Fig. 5 (but averaged over only 2000 runs), using the same color code. As detailed in the text, the initially solution of labeled proteins (with concentration $c = 0.2$) was replaced at time $2/v$ by either a buffer solution (solid lines), or an "unlabeled" solution of the same concentration (densely dashed lines), or a more concentrated unlabeled solution (sparsely dashed lines). For comparison, we have also plotted the total surface density ρ in the infinite diffusion limit with buffer replacement (upper dotted line), as well as in the limit of the fastest exchange (i.e., when no spreading of the labeled proteins is allowed) (lower dotted line). (b) Caricature of the "ratcheting" mechanism of protein exchange.

binding conditions and the protein concentration. We have also predicted the existence of a well defined transition between predominantly compact and expanded states in the adsorbed layer as a function of either the concentration or the binding conditions.

Introducing dynamics, we derived an analytically tractable mean field model, which is equivalent to the limit of infinite surface diffusion of the adsorbed proteins. We have also performed direct MC simulations of the zero diffusion dynamics, and have been able to qualitatively reproduce several experimental phenomena. The comparison between the mean field model and the MC simulations underpins the importance of RSA like surface frustration in the slowing down of the adsorption dynamics. The MC simulations have also led us to the idea of a novel experimental method for the study of protein exchange.

Acknowledgements

Appendix A. Configurations on a continuous line

Starting from a continuous model where each adsorbed protein is located along a continuous line (1D surface) of adsorption, approximation (8) can be shown to be exact in the $\delta \to 0(n_0 \to \infty)$ limit. To arrive at this result, directly the continuous configuration volume $\mathscr{C}(\{n_i\})$ has to be derived.

Let us first consider only one adsorbed protein ($N = 1$) in state i. This protein separates the adsorption surface into two disjunct intervals,[4] each of which can have a length of maximum $L - l_i$. For arbitrary N, each of the $N + 1$ intervals has a length

$$w_j \in [0, L - l], \quad \text{where} \quad j \in \{1, 2, \ldots, N + 1\} \tag{A.1}$$

with l being the total occupied surface. The intervals w_j must also satisfy the spatial constraint

$$\sum_{j=1}^{N+1} w_j = L - l \,. \tag{A.2}$$

This means that the configuration volume $\mathscr{C}(\{n_i\})$ for a single protein is simply the length of the hypotenuse of a right triangle with legs of equal length, $L - l$ (Fig. 7a).

For $N = 2$, $\mathscr{C}(\{n_i\})$ is the area of the equilateral triangle base of the pyramid formed by the origin, $(L - l, 0, 0)$, $(0, L - l, 0)$, and $(0, 0, L - l)$ in the 3D space of w_1, w_2 and w_3 (Fig. 7b). So far we have considered the adsorbed proteins indistinguishable—by only considering the lengths and arrangement of the empty intervals, but not the order of the adsorbed proteins—, consequently this area has to be multiplied by a factor of two when the proteins are in different states.

In general for $N > 2$ the configuration volume is an N-dimensional hyper-surface in the $N + 1$-dimensional space of w_j-s defined by the constraint (A.2), multiplied by a factor of $N!/\prod_{i=1}^{M} n_i!$ This can be written in an integral form as

$$\mathscr{C}(\{n_i\}) = \frac{N!}{\prod_{i=1}^{M} n_i!} \int_{-\infty}^{\infty} \prod_{j=1}^{N+1} \mathrm{d}w_j \prod_{j=1}^{N+1} \Theta(w_j) \delta\left(L - l - \sum_{j=1}^{N+1} w_j\right), \tag{A.3}$$

---

[4]This separation of intervals (or shielding property) only holds in 1D, which is one of the main reasons that 2D calculation are far more difficult.
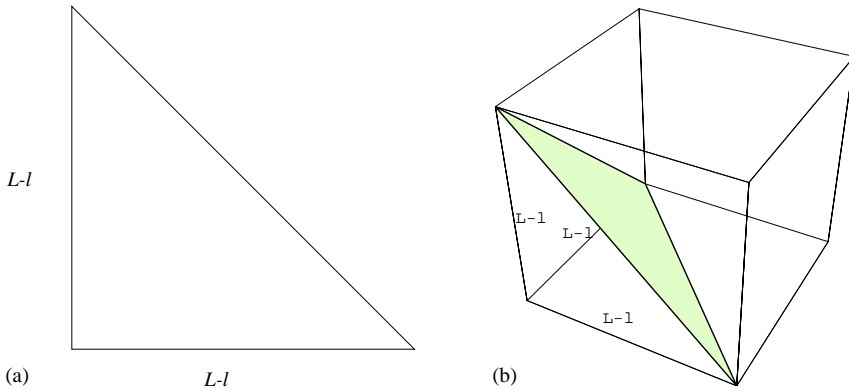
Fig. 7. $\mathscr{C}(\{n_i\})$ for (a) $N = 1$ and (b) $N = 2$.

where $\Theta(x)$ is the Heaviside function. Carrying out the integration with respect to w_{N+1} we have

$$\int_{-\infty}^{\infty} dw_{N+1} \ \Theta(w_{N+1}) \ \delta\left(L - l - \sum_{j=1}^{N+1} w_j\right) = \Theta\left(L - l - \sum_{j=1}^{N} w_j\right). \tag{A.4}$$

Integrating again with respect to w_N:

$$\int_{-\infty}^{\infty} dw_N \ \Theta(w_N) \ \Theta\left(L - l - \sum_{j=1}^{N} w_j\right)$$

$$= \left(L - l - \sum_{j=1}^{N-1} w_j\right) \ \Theta\left(L - l - \sum_{j=1}^{N-1} w_j\right). \tag{A.5}$$

Now we can see that by integrating with respect to the remaining $N - 1$ variables one by one in a similar way, we arrive at

$$\mathscr{C}(\{n_i\}) = \frac{(L - l)^N}{\prod_{i=1}^{M} n_i!}, \tag{A.6}$$

which, divided by the unit volume δ^M, is the same as Eq. (7) with the approximation (8), which can now be considered exact in the $\delta \to 0$ limit.

References

[1] C. Calonder, Y. Tie, P.R. Van Tassel, Proc. Natl. Acad. Sci. USA 98 (2001) 10664.
[2] W. Norde, Cells Mater. 5 (1995) 97.
[3] J. Bujis, W. Norde, J.W.T. Lichtenbelt, Langmuir 12 (1996) 1605.
[4] C.F. Wertz, M.M. Santore, Langmuir 15 (1999) 8884.
[5] W. Norde, W.J.P. Favier, Colloids Surfaces 64 (1992) 87.
[6] J. Talbot, G. Tarjus, P.R. Van Tassel, P. Viot, Colloids Surfaces A 165 (2000) 287.
[7] W. Norde, J. Disper. Sci. Technol. 13 (1992) 363.

[8] W. Norde, in: A. Baszkin, W. Norde (Eds.), Physical Chemistry of Biological Interfaces, Marcel Dekker, New York, 2000, p. 115.

[9] I. Lündstrom, Prog. Polymer Colloid Sci. 70 (1985) 76.

[10] P.R. Van Tassel, P. Voit, G. Tarjus, J. Chem. Phys. 106 (1996) 761.

[11] C.F. Wertz, M.M. Santore, Langmuir 18 (2002) 1190.

[12] C.F. Wertz, M.M. Santore, Langmuir 18 (2002) 706.

[13] P.R. Van Tassel, Materialwiss. Werkst. 34 (2003) 1129.

[14] G.J. Fleer, M.A. Cohen-Stuart, J.M.H.M. Scheutjens, T. Cosgrove, B. Vincent, in: G.J. Fleer, M.A. Cohen Stuart, J.M.H.M. Scheutjens (Eds.), Polymers at Interfaces, Kluwer Academic Publishers, Dordrecht, 1993.

[15] V. Ball, P. Schaaf, J.-C. Voegel, Surfactant Sci. Ser. 110 (2003) 295.

[16] E. Ostuni, B.A. Grzybowski, M. Mrksich, C.S. Roberts, G.M. Whitesides, Langmuir 19 (2003) 1861.

[17] M.C.L. Martins, B.D. Ratner, M.A. Barbosa, J. Biomed. Mater. Res. 67A (2003) 158.

[18] C. Brunner, Diploma Thesis: Immunoglobulin G immobilization on PLL-g-PEG modified titanium oxide surfaces, ETH Zurich, 2003.